

Regular Paper

## Controlled Vortex Breakdown on Modified Delta Wings

Srigrarom, S.\* and Lewpiriyawong, N.\*

\* School of Mechanical and Aerospace Engineering, Nanyang Technological University, 50 Nanyang Avenue, 639798, Singapore. E-mail: mssrigrarom@ntu.edu.sg

Received 30 October 2006  
Revised 14 March 2007

**Abstract** : This paper studies the effect of perturbation to the breakdown of the leading-edge vortices over delta wings. The passive perturbation in the normal direction is achieved by installing the hemisphere-like bulges on the delta wing along the projection of the vortices. The key purpose of this perturbation is to delay or suppress vortex breakdown over delta wings according to the self-induction mechanism theory. The design of bulge-like surface for delta wings offers a minimization of initial vorticity gradient and an elimination of linearly mutual induction within the vortex core. Three delta wings with swept angles of 60°, 65° and 70° have been used. Dye flow visualization and force measurement in different water tunnels are performed at the water speed of  $U = 0.10, 0.15, 0.20$  and  $0.25$  m/s. In flow visualization, the results show contributions of bulges as perturbation to leading-edge vortices. The best outcome of perturbing the vortex core occurs in the case of the 65° delta wing. The breakdown positions on the 65° delta wing are delayed in almost the entire range of angles of attack, and that, the results are presented here.

**Keywords** : Vortex breakdown, Delta wing, Bulge perturbation.

### 1. Introduction

This study focuses on the flow visualization of the delta wing with and without modification for comparing and illustrating the controlled and uncontrolled vortex breakdown, resulted from the modified and unmodified delta wing.

The concept of this study is based on the self-induction theory proposed by Srigrarom and Kurosaka (2000a) and by Srigrarom and Kurosaka (2000b) which states that the existence of negative vorticity gradient and the initial straightness of apex vortex are two important keys leading to Leading-edge vortex (LEV) breakdown. This theory explains that the self-induction in the shear layers spiraling around the vortex core causes the accumulation of vorticity, which in turn induces backflow and radial enlargement of stream surfaces. The process starts as the axial vorticity of the LEV induces azimuthal velocity, and in turn tilts the vorticity vector in the azimuthal direction. Due to the gradient in azimuthal vorticity caused by the increase in circulation, the vortex tube radial expands and the vortex filaments contract in an action called “pile-up”. This is followed by a sign switch in the azimuthal vorticity vector caused by the region downstream of the vorticity gradient rotating slower than the region upstream of the gradient. These actions proceed together until they form a point where the vortex filaments turn inward on themselves. These inwards vortex filaments sustain the radial expansion and azimuthal vorticity sign switching process, and that the flow eventually becomes vortex breakdown.

At the beginning, we investigated the influence of the initial straightness of LEV perturbing the vortex core close to the apex. The vortex filament method was used in this simulation (Leonard,

1980). This method examines the development of vortex filaments. It solves (1) vorticity equation for the new distribution of vorticity as time goes on, and (2) Biot-Savart law for induced velocity to change the positions of all vortex filaments. The details of this simulation work can be found in Srigrarom 2003.

To satisfy the asymmetrically transient formation of vortex breakdown in the real situation, the asymmetric condition of apex vortices in our computation is considered to be crucial. The asymmetrically simulative results are found obviously that the initial straightness of LEV as predicted by self induction theory is a trigger to the vortex breakdown phenomena. In turn, after introducing perturbation to the system, diffusion in some cases of simulation exists instead of breakdown yet for some situations breakdown can be delayed.

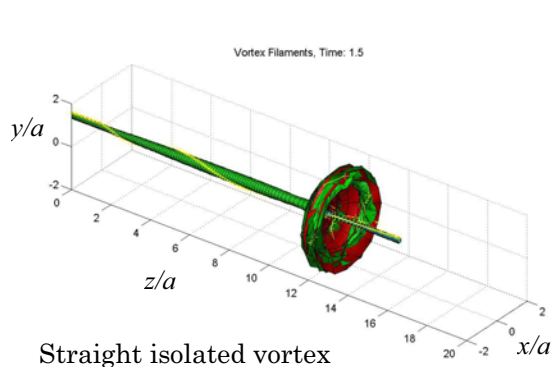


Fig. 1. Straight isolated vortex from computer simulation, based on vortex filament method, which later breaks down. The units are distance/initial vortex core size ( $a$ ).

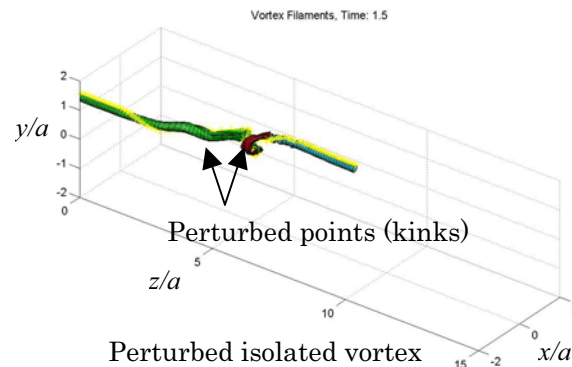


Fig. 2. Perturbed isolated vortex from computer simulation, based on vortex filament method.

Figure 1 shows the simulation of the isolated vortex (which is representing apex vortex) based on vortex filament method. The units of the axes are distance/initial vortex core size ( $a$ ). This vortex undergoes breakdown, at certain time ( $\tau = 1.5$  where  $\tau \equiv t \cdot a / U_\infty$ ), as clearly indicated by rapid radial enlargement. On the contrary, Fig. 2 shows the simulation of the similar isolated vortex but with perturbation as noticeable by the two kinks to the left of the knot. At the same time,  $\tau = 1.5$ , this vortex does not breakdown, instead, it forms a knot and be carried downstream.

It should be noted here that, the vortex breakdown phenomenon is well known and well studied as inviscid process (e.g., Althaus et al., 1996; Hall, 1972), i.e., independent of Reynolds number. Although, the flow conditions are different, the key physical mechanism to be presented in this paper remains the same in every flow conditions (speeds). Therefore, the results of the present study can be applicable to the real flow around the actual full-size delta wing aircraft.

## 2. Dye Flow Visualization

Flow visualization experiments are very beneficial in an investigation of flows over a delta wing especially in low speeds. The flow visualization exploits the concept of a streak line which describes all locations of fluid particles coming out from the fixed point in an interval of time. In this present work, a pair of leading-edge vortices stemming from the apex of the delta wing is made visible by using food coloring dye. The highlight is the visualization of the unperturbed and perturbed delta wing with bulges. The results and comparisons of experiment cases are shown in this section. These experiment results will show the effectiveness of methodology of suppressing vortex breakdown by shaping the delta wing's surface to be like bulge-like.

The flow visualization experiments are performed in the recirculating water tunnel at Nanyang Technological University (NTU) in Singapore. The cross section of water tunnel is 0.45 x 0.6 meter square and the length of the test section is 1 meter. The water tunnel turbulence intensity is < 1 % RMS at speed >0.02 m/s. The speed of 5 cm/s is chosen for all cases in visualization experiment. The Reynolds number based on chord length is of 15,000. Three plain delta wings with different

sweep back angles are used in flow visualization experiments. The  $60^\circ$ ,  $65^\circ$  and  $70^\circ$  sweep back angles ( $\Lambda$ ) are chosen. All of them have the same chord length of 30 centimeters.

### 2.1 Dye Flow Visualization of the Vortex Breakdown

Firstly, we examine the flow visualization images of the vortex breakdown itself. Figure 3 shows the  $65^\circ$  swept angle delta wing at  $30^\circ$  angle of attack under freestream velocity of 5 cm/s. The food coloring dye was released at the apex of the wing. This dye shows the two vortices emanated from the apex and broken down on both sides. Figure 4 shows the zoomed-in image of this vortex breakdown. Figure 5 shows the flow surrounding the apex vortex (red dye) wrapping around the apex vortex (blue dye). This red dye represents the conical vortex sheet caused by the separated flow from the side of the delta wing. This conical vortex sheet wraps around the apex vortex (shown in blue), and acts like a tube to prevent the apex vortex not to grow radially. In this regard, the vortex breakdown on delta wing is analogous to vortex breakdown in pipe. Figure 6 is the two-dimensional cross-sectional view in the meridional plane of vortex breakdown –taken by Laser Induced Fluorescence (LIF) technique. The back flow can be identified by the accumulation of the dye inside the enlarged vortex core and there is vortex ring formed around it. As shown in these figures, the sudden enlargement of the vortex and the existence of the backflow at the vortex center are the indication of the vortex breakdown. The details discussion can be found in references (Srigarom and Kurosaka, 2000a; Srigarom and Kurosaka, 2000b).

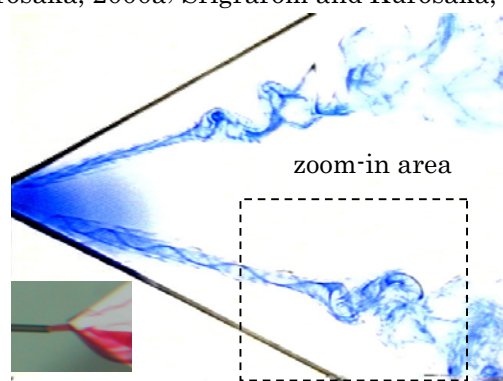


Fig. 3. Side view of the  $65^\circ$  swept delta wing with vortex breakdown.



Fig. 4. Zoom-in of the apex vortex breakdown (from the area shown in Fig. 3).



Fig. 5. The apex vortex breakdown (blue) wrapped around by the surrounding flow (red).

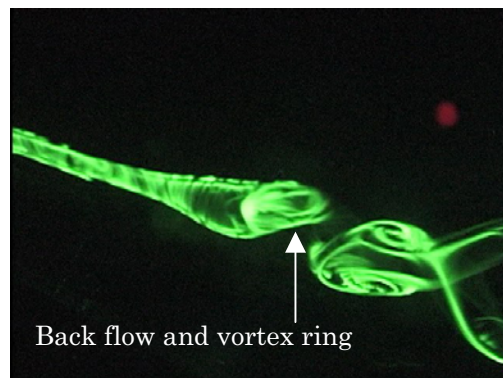


Fig. 6. The two-dimensional cross-sectional view in the meridional plane of vortex breakdown –taken by Laser Induced Fluorescence (LIF) technique.

### 2.2 Dye Flow Visualization of the Delta Wing's Apex Vortices.

This visualization experiment emphasizes on the leading-edge vortices emanating from a delta wing. Cases of experiment are categorized into two parts. The first part of experiment is to visualize the pair of the unperturbed leading-edge vortices, and the second part is to investigate the behavior of

the perturbed leading-edge vortices over a delta wing. To be convenient to compare both cases, the delta wing's surface is divided into two zones. The example of modification to the  $70^\circ$  delta wing's surface is illustrated in Fig. 7. The size of the small hemisphere-like bulge is 12 millimeters in diameter and 3.7 millimeters in height. As for the big bulge, its diameter is 15 millimeters and its height is 4 millimeters. The objective of installing the bulges on the delta wing surface is to perturb the apex vortices to deviate from the straight tline. Therefore, the bulges are installed on the delta wing surface and in line with the projection of the trajectory of the apex vortices on the delta wing surface. With the aid of the flow visualization results in Table 1, we follow the projection of the apex vortices trajectory accordingly. They are also approximately located half way between the delta wing's centerline and the leading edges. Since the position of perturbation should be close to the apex to reduce the initial vorticity gradient and cancel the linearly mutual induction along the apex vortex, the small bulge and big bulges are located on the suction side at 4 and 6 centimeters along the root chord length. Several researchers (e.g., Bean and Wood, 1996; Guy et al., 1999) also tried to suppress the vortex breakdown near the apex. It is noted that the  $60^\circ$ ,  $65^\circ$  and  $70^\circ$  delta wings with the 30-cm root chord and bulges are also used in the force measurement which will be discussed in the next section, so these experiments complement to each other. In experiment, the range of angles of attack is from 20 to 35 degrees.

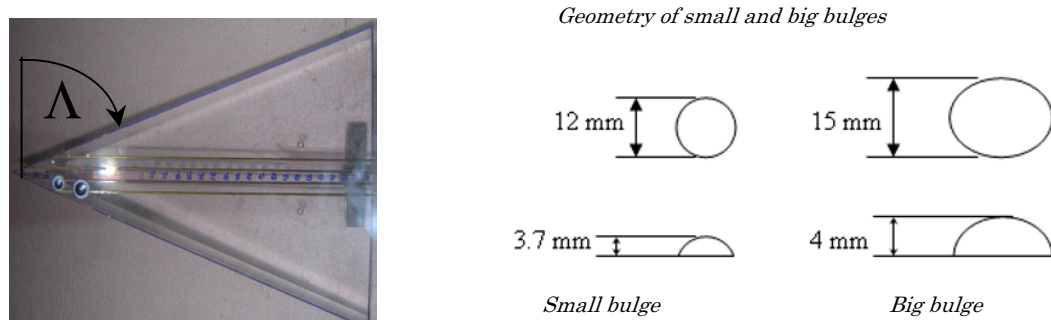


Fig. 7. The release of the dye at the apex of the delta wing, and the modification of delta wing's surface with bulges and geometry of small and big bulges.

It should be noted that the bulges were installed and stayed on the wing for the whole tests. Therefore, there was no temporal frequency of perturbation with time. However, we can consider there is spatial frequency of perturbation with space, since the bulges were located along the projection of the vortex trajectory. If we define,  $f = 1/T$ , and  $T = x/U_\infty$  where  $x$  is the space between the bulges, and  $U_\infty$  is the freestream velocity, our spatial frequencies  $f$  are 2.5, 5.0, 7.5, 10 and 12.5 Hz, for  $x = 2$  cm,  $U_\infty = 5, 10, 15, 20$  and  $25$  cm/s respectively (our bulges were installed at 4 cm and 6 cm from the apex, as shown in Fig. 7). Note also that, the bulges are of circular shape. This is to mimic the shape of the conventional actuator or diaphragm, or blowing/suction port(s), for vortex breakdown control.

From experiments, the position of breakdown of the unperturbed apex vortex on delta wing at a fixed angle of attack cannot be fixed but can be specified its range of fluctuation in terms of percentage of the root chord. The fluctuation in this experiment is 8 % of root chord. The root chord of three delta wings is 30 cm, so 8 % of the root chord equals 2.4 cm. This number was always found in experiment and can be supported by the results in Fig. 8. Cameron et al. (2003) also found the vortex breakdown fluctuation over delta wings. In their work, all observed locations of vortex breakdown at an angle of attack were recorded and presented in terms of the fluctuating range of vortex breakdown.

The flow visualization of flow over three delta wings are summarized in tables 1, 2 and 3 for delta wings with swept angle ( $\Lambda$ ) =  $70^\circ$ ,  $65^\circ$  and  $60^\circ$  respectively. Some similarities in experiment results are found as follows. Firstly, the initial straightness of leading-edge vortices' core is interfered to become wavy. This is obviously seen in the cases of the  $60^\circ$  and  $65^\circ$  delta wing with a bulge at 25 angles of attack. Secondly, the vortex breakdown positions do not stand still in a fixed place but fluctuating in nature. Note that, the fluctuations in positions of the vortex breakdown have been reported by many researchers, e.g. as reported in Hall (1972). Here, we recorded all the tests by

means of video camera for more than 1 minute in each test, and that, we also observed these positional fluctuations. The results shown in Figs. 3-6 are from our Nikon Digital SLR camera, of which the camera shutter's duration was the standard 1/20 second.

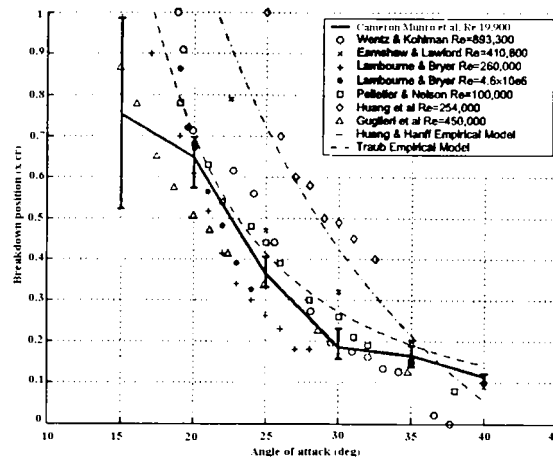


Fig. 8. Vortex breakdown position of  $65^\circ$  delta wing, from Cameron et al. (2003).

As for the effect of bulges on a surface, the visualization results reveal that the  $60^\circ$  and  $65^\circ$  delta wings can gain the benefit of perturbation to delay the vortex breakdown in almost the entire range of angles of attack. However, some visualization results do not obviously show the occurrence of vortex breakdown. Instead, diffusion perhaps does happen, but the lack of equipment such as PIV to confirm the results limits further analyses on the back flow which represents vortex breakdown. These suspicious locations of diffusion can be seen at high angles of attack, 30 and 35 degrees, in the case of the  $65^\circ$  and the  $70^\circ$  delta wing with 2 bulges.

In parallel to top view images as shown above, we also conducted flow-visualization experiments on delta wing with and without bulges from edge view. Note that, the role of the bulges on the delta wing suction surface is still to perturb the apex vortices from straight one. In this paper, we define the vortex breakdown from flow visualization images by (1) the sudden enlargement (increase in radius) of the vortex column, (2) the presence of the back flow and (3) the sudden and significant drop in axial vorticity, which results in the slow down of the spinning of the tail downstream of the vortex breakdown. This definition is the same as Hall (1972). Figure 9 shows the side view flow coloring dye flow visualization of the unperturbed (straight) apex vortex on the  $65^\circ$  degrees swept angle and 30 cm delta wing at 15 degrees angle of attack, which undergoes breaking down process. Figure 10 shows the same wing, but with two 2 cm diameter and 5mm thick bulges (one on each side, appeared in black) installed. After passing the bulge, the vortex just turns around. Although the vortex column appears to be bigger, there is no obvious accumulation of dye for being interpreted as the backflow. The spinning motion of the downstream flow behind is also relatively the same as the upstream one. Therefore, the corresponding apex vortex is perturbed by the bulges and hence, does not breakdown, instead, it forms a knot and diffuses away.

We also conducted flow-visualization experiments on delta wing with concave and convex leading edges, as shown in Figs. 11 and 12. (The closed-up looks are shown in Figs. 13 *a*, *b*, *c* and *d*) This is to compare the initial vorticity gradient, created by the turning motion of the flow at the delta wing's edge. The strength of the vorticity gradient depends upon the wing's sharpness. With concave leading edge delta wing as shown in Fig. 11, the incoming flow will follow the gentler turn with larger radius to form the milder apex vortex (with less initial vorticity). On the contrary, with the convex leading edge as shown in Fig. 12, the incoming flow will follow the abrupt turn with smaller radius to form the stronger apex vortex (with more initial vorticity). The blunt convex-edge-delta wing shows no trace of vortex breakdown. The separated flow just convected and diffused downstream as shown in Fig. 11. From the side view, these apex vortices are straight and breakdown consequently as shown in Fig. 12. Both blunt convex-edge and sharp concave-edge were tested in water tunnel at 10 cm/s freestream and the wings were at 20 degrees angle-of-attack. Based on this observation, this also agrees to the proposed self-induction theory that the vorticity gradient and the initial straightness causes slender vortex to breakdown.

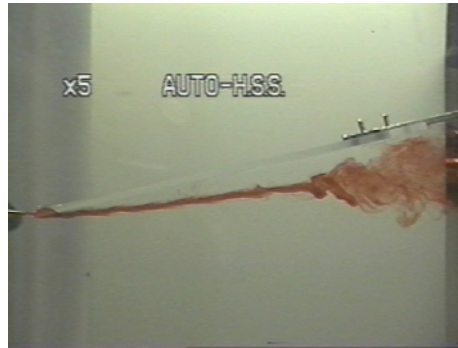


Fig. 9. The side view of the unperturbed (straight) apex vortex on  $65^\circ$  swept delta wing at  $15^\circ$  deg. angle of attack. The vortex breakdown clearly appears.

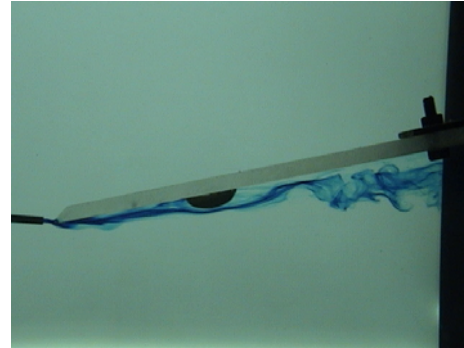


Fig. 10. The side view of the same wing as in Fig. 9 at the same condition, but with two bulge perturbations. The apex vortex just turns and does not break down.

(From the Figs. 11 and 12, we can see the larger and smaller turning radii at the apexes of the delta wings. These are the indications of the initial vorticities of the apex vortices on both wings  $\omega(z=0) = \omega_0 > 0$ . Since, along downstream there is no further creation of vorticity  $\omega(z > 0) = 0$ , therefore, along the vortices' axial directions, there are vorticity gradients in the apex vortices  $\partial\omega/\partial z \neq 0$  in both cases.)

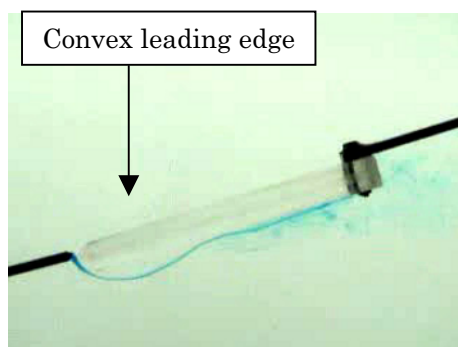


Fig. 11. Side-view of the delta wing with blunt convex leading edge in  $10 \text{ cm/s}$  water flow at  $20^\circ$  degrees angle of attack. From this dye flow visualization, no apex vortex appears.

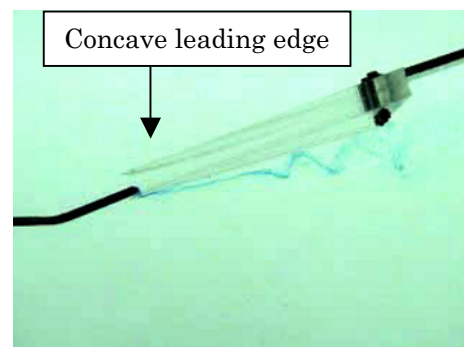


Fig. 12. Side-view of the delta wing with sharp concave leading edge in the similar flow situation. The apex vortices exist and break down.

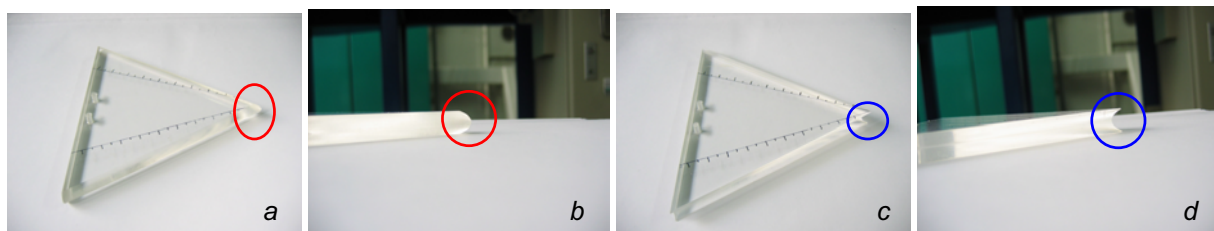


Fig. 13. a, b: Convex delta wing used (a: 3-D photo, b: edge-view photo); c, d: Concave delta wing used (c: 3-D photo, d: edge-view photo).

Table 1. The visualization results of the 70° delta wing (Chord length = 30 cm).

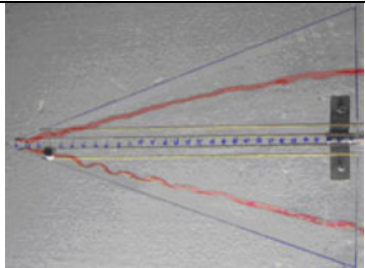
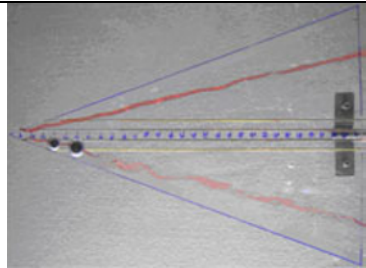
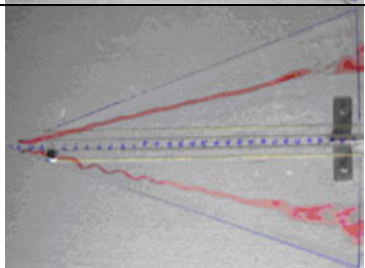
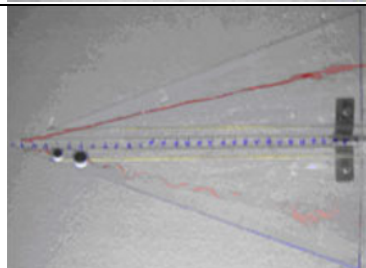
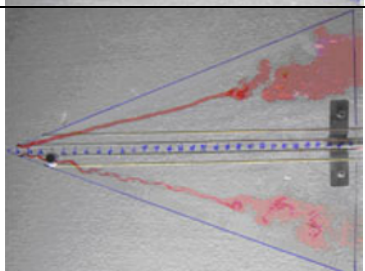
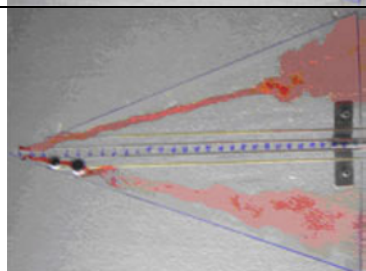
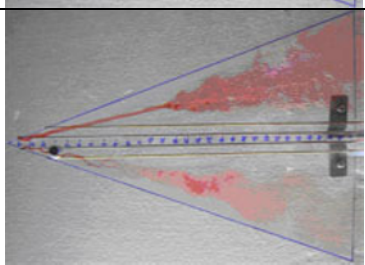
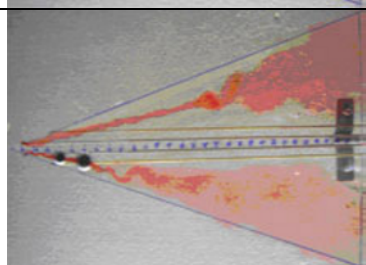
AoA (degrees)	Case I: a small bulge located at 4 mm or 1.3 % chordwise	Case II: 2 bulges located at 4 and 6 mm or 1.3 % and 2 % chordwise
20		
25		
30		
35		

Table 2. The visualization results of the 65° delta wing (Chord length = 30 cm).

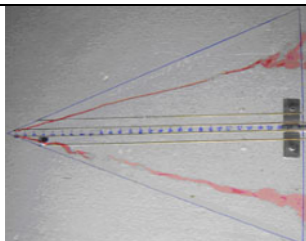
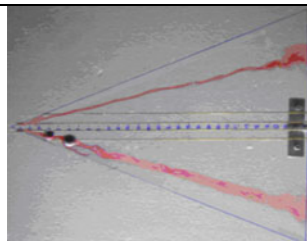
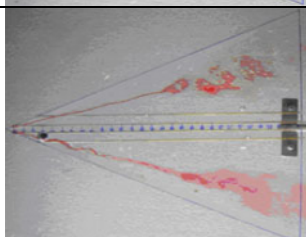
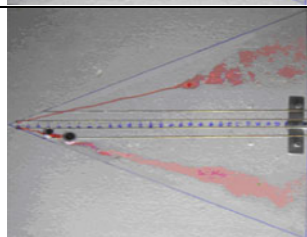
AoA (degrees)	Case I: a small bulge located at 4 mm or 1.3 % chordwise	Case II: 2 bulges located at 4 and 6 mm or 1.3 % and 2 % chordwise
20		
25		

Table 2. (Continued).

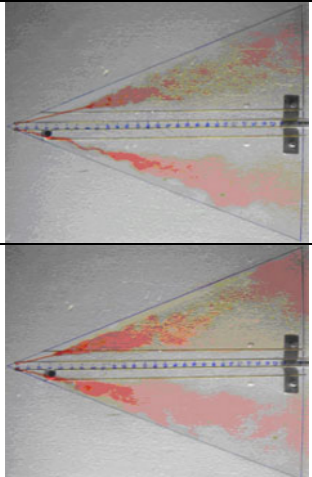
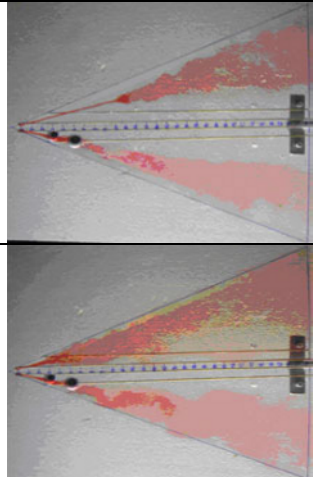
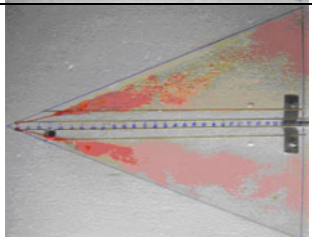
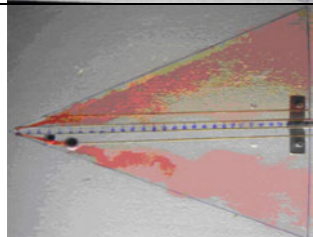
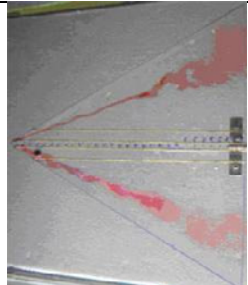
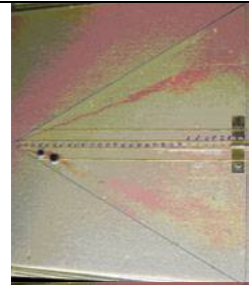
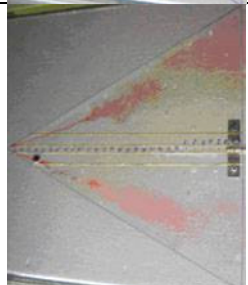
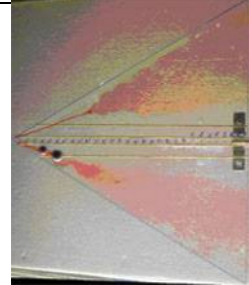
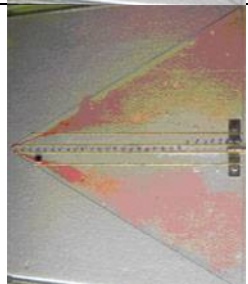
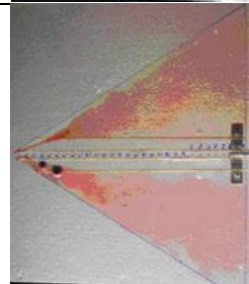
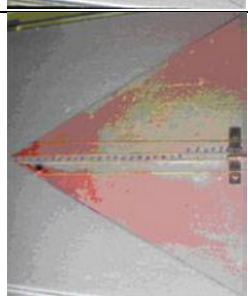
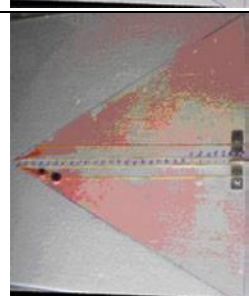
30		
35		

Table 3. The visualization results of the 60° delta wing (Chord length = 30 cm).

AoA (degrees)	Case I: a small bulge located at 4 mm or 1.3 % chordwise	Case II: 2 bulges located at 4 and 6 mm or 1.3 % and 2 % chordwise
20		
25		
30		
35		



### 3. Conclusion

Vortex breakdown, an important lift killer, occurs over delta wings' planform as angles of attack increase to a critical angle, depending on the sweep back angle. The proposed self-induction mechanism theory states that a negative vorticity gradient and an initial straightness of vortex core are key factors causing the pile-up, radial expansion, azimuthal vorticity sign switch, leading the apex vortex to breakdown eventually. The current design of surface modification based on the self-induction mechanism theory is to shape the surface in the vicinity of apex to be hemisphere-like bulge. This hemisphere-like bulge design on delta wing's surface offers both a minimization of initial vorticity gradients and a cancellation of linearly mutual inductions due to the wavy pattern of the vortex core. The flow visualization results show contributions of bulges as perturbation to leading-edge vortices. The best outcome of perturbing the vortex core occurs in the case of the 65° delta wing. According to the results, the breakdown positions on the 65° delta wing are delayed in almost the entire range of angles of attack. Since this vortex breakdown mechanism is inviscid process, i.e. independent of Reynolds number, the results of the present study can be applicable to the real flow around the actual full-size delta wing aircraft. The limitation will probably be more on energy consumption/space constraints, etc. than fluid mechanics and/or aerodynamic issue, for example: how much energy to activate the actuator, where to install the actuator on the wing, etc. If these non-aerodynamic related problems have been solved or taken care of properly, the application on the real aircraft at high Reynolds can be realized. To sum up, from the results obtained by flow visualization the proposed current methodology to suppress vortex breakdown is clearly effective for many situations over delta wings.

### References

- Althaus, W. and Brucker, Ch. And Weimer M., Breakdown of slender vortices, in Green, S. I. (ed.), Fluid Vortices, (1996), 373-426, Kluwer Publishers, Netherlands.
- Bean, D. E. and Wood, N. J., An experimental investigation of twin fin buffeting and suppression, *Journal of Aircraft*, 33-4, (1996), 761-767.
- Cameron, M., Christopher, J. and Petter, K., Flow visualization and Force and Moment correlations in a water tunnel, 7th International Symposium on Fluid Control, Measurement and visualization, (2003).
- Guy, Y., Morrow, J. and McLaughlin, T., Control of Vortex Breakdown on a Delta Wing by Periodic Blowing and Suction, 37th AIAA Aerospace Sciences Meeting (Reno NV), AIAA 99-0132, (1999-1).
- Hall, M. G., Vortex breakdown, *Annual Review of Fluid Mechanics*, 4 (1972), 195-218.
- Leonard, A., Vortex Methods for Flow Simulation, *Journal of Computational Physics*, 37 (1980), 289-335.
- Srigarom, S. and Kurosaka, M., Shaping of Delta-wing Planform to Suppress Vortex Breakdown, *AIAA Journal*, 38-1 (2000a), 183-186.
- Srigarom, S. and Kurosaka, M., Surface Shaping to Suppress Vortex Breakdown on Delta Wings, *AIAA Journal*, 38-1 (2000b), 186-187.
- Srigarom, S., Transient Vortex Breakdown Formation Simulation by Vortex Particle Method, *Computational Fluid Dynamics Journal (CFDJ)*, 12-1 (2003-4), 65-79.

### Author Profile



Sutthiphong Srigarom: He received his M.Sc. in Aeronautics and Astronautics in 1998, and his Ph.D. in 2001, both from University of Washington, Seattle, USA. In 2002, he joined Nanyang Technological University (NTU), School of Mechanical and Aerospace Engineering in Singapore, as an assistant professor in aeronautical engineering. At NTU, he is in charge of water channels and wind tunnel lab facilities. His current research interests are Vortex Dynamics, Flow Visualization (both qualitative and quantitative), PIV, and Flow-Induced Vibration.



Nuttawut Lewpiriyawong: He received his B.Eng. in Mechanical Engineering in 2001 from King Mongkut's Institute of Technology Ladkrabang (KMUTL), Thailand, and his M.Eng. in Mechanical Engineering from Nanyang Technological University (NTU) in 2006. Currently, he is doing Ph.D. in Mechanical Engineering in Nanyang Technological University (NTU). His interests are Vortex Dynamics, Flow visualization, and Microfluidic.